Unpinning and Removal of a Rotating Wave in Cardiac Muscle

S. Takagi,[1] A. Pumir,[1,*] D. Pazó,[1] I. Efimov,[2,†] V. Nikolski,[2] and V. Krinsky[1]

[1]*Institut Non Linéaire de Nice, 1361 route des Lucioles, F-06560, Valbonne, France*

[2]*Biomedical Engineering, Case Western Reserve University, Cleveland, Ohio 44106-7207, USA*

(Received 5 January 2004; published 26 July 2004)

Rotating waves in cardiac muscle may be pinned to a heterogeneity, as it happens in superconductors or in superfluids. We show that the physics of electric field distribution between cardiac cells permits one to deliver an electric pulse exactly to the core of a pinned wave, without knowing its position, and even to locations where a direct access is not possible. Thus, unpinning or removal of rotating waves can be achieved. The energy needed is 2 orders of magnitude less than defibrillation energy. This opens a way to new manipulations with pinned vortices both in experiments and in cardiac clinics.

DOI: 10.1103/PhysRevLett.93.058101 PACS numbers: 87.19.Hh, 87.50.Rr

Rotating waves, or vortices, are ubiquitous in physics. The dynamics underlying fluid turbulence is ultimately related to the motion of vortices [1]. Vortices also play a crucial role in condensed matter physics. In superconductors, the motion of free vortices induces dissipation, so pinning is required to maintain the superconducting state [2]. Pinning and depinning transitions are essential features of dynamics of superfluids [3,4] and Bose-Einstein condensates [5] .

The turbulent regime of electrical activity (fibrillation) leading to life threatening cardiac arrhythmias results from the dynamics of vortices evolving in the heart. Controlling cardiac chaos is often achieved by applying a large damaging electric shock defibrillation (~ 5 kV, or ~ 100 V directly to cardiac muscle). It removes all waves, without differentiating vortices and normal waves.

Vortices in the heart may be free or their cores may be pinned to a heterogeneity. Pinned vortices (anatomical reentries) are usually removed by delivering a gentle electric pulse or train of pulses ~ 1 V (antitachycardia pacing, ATP). The success rate of ATP is 60%–90% only [6]; it is low when the intracardiac catheter with a stimulating electrode is situated far from the core of the pinned vortex.

We demonstrate in this Letter that applying a uniform electric field of weak intensity across the heart is sufficient to unpin or remove the rotating wave. The effect rests on the response of cardiac tissue to an external electric field that modifies the membrane potential mainly near the obstacles (at the boundaries of the tissue). The analysis is carried out using the well-known bidomain model [7], which is a macroscopic model that describes the average electric potential in two domains: inside and outside the cardiac cells. Of interest is the spatial distribution of difference between the two domains, i.e., the potential difference across the idealized average ''membrane.'' The model's derivation rests on a multiscale analysis (the cells are much smaller than the typical scale of variation of the electric properties inside the medium). Importantly, the anisotropies in the conductivities of the medium are correctly described by the bidomain model. The bidomain model successfully describes the influence of a strong electric field in cardiac tissue, in particular, the pattern of electrical activity after an intense point current injection in the tissue; see Fig. 1(b).

We show analytically and numerically that the current applied across an obstacle creates a membrane potential distribution that consists of a dipolar term, superimposed with an hexapolar term (Fig. 1). We demonstrate that this effect can be used to unpin a rotating wave (Fig. 2). The energy required to unpin is reduced compared to the energy used to defibrillate by 2 orders of magnitude.

The bidomain model describes the extracellular potential, ϕ_e, and the intracellular potential, ϕ_i

$$\nabla \cdot \sigma_i \nabla \phi_i = \beta \left[C_m \frac{\partial}{\partial t}(\phi_i - \phi_e) + I_{\text{ion}} \right] - I_i, \quad (1)$$

$$\nabla \cdot \sigma_e \nabla \phi_e = -\beta \left[C_m \frac{\partial}{\partial t}(\phi_i - \phi_e) + I_{\text{ion}} \right] - I_e, \quad (2)$$

where σ_i and σ_e are the conductivity tensors, I_i and I_e are the currents coming from external sources, injected in the intracellular and extracellular spaces, respectively. β and C_m are parameters; I_{ion} is the ionic current.

We begin by considering the steady membrane potential distribution around an obstacle with an applied extracellular uniform current, I_e. For a weak field, the equations can be linearized $I_{\text{ion}} = G_m V_m$, where the membrane potential $V_m = \phi_i - \phi_e$, and read

$$\nabla \cdot (\sigma_e \nabla \phi_e) = -\beta G_m V_m - I_e, \quad (3)$$

$$\nabla \cdot ((\sigma_e + \sigma_i)\nabla \phi_e + \sigma_i \nabla V_m) = 0. \quad (4)$$

The conductivity tensors in the extra (intra) cellular medium σ_e (σ_i) are anisotropic, reflecting the existence of long fibers in the tissue. The analysis is restricted to 2 dimensions. We consider a circular obstacle of radius R, consisting of ischemized cells ($G_m = 0$), mutually uncoupled ($\sigma_i = 0$). Let σ_e be isotropic: $\sigma_e = \Sigma_e \mathbf{I}$. The σ_i outside of the obstacle is written as

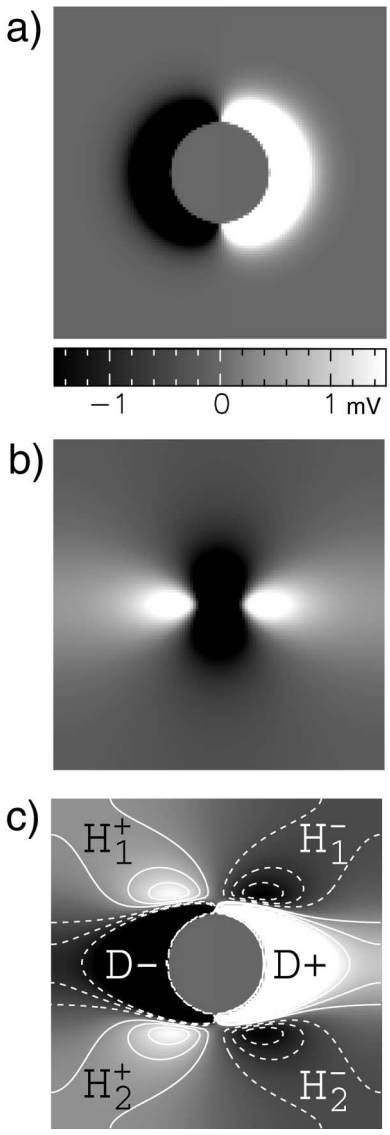

FIG. 1. Patterns induced by an electric field in cardiac tissue: (a) dipole; (b) quadrupole; (c) hexapole. (a) an obstacle 6 mm diameter, anisotropy ratio $a = 1$, $E = 0.2$ V/cm. (b) point injection of current $I = 1.8$ μA, $a = 10$. (c) same as in (a), $a = 10$. Contours drawn at intervals of 0.4 mV. Bidomain model, $G_m = 0.165$ mS/cm^2, $\sigma_{ex} = \sigma_{ey} = \sigma_{ix} = 14.4$ mS/mm, $\sigma_{iy} = 1.44$ mS/mm, $\beta = 2000$ cm^{-1}.

$\sigma_i = \Sigma_i \begin{pmatrix} 1+\epsilon & 0 \\ 0 & 1-\epsilon \end{pmatrix}$. The anisotropy ratio is defined by $a \equiv (1+\epsilon)/(1-\epsilon)$. The discontinuity of σ_i across the obstacle boundary imposes a separate treatment inside and outside the obstacle. Inside, the membrane potential is undefined, and the continuity conditions for the potential and for the currents must be written. Away from the obstacle, a uniform current $[I_e = I_0(\theta)]$ is imposed; $V_m \to 0$ when $r \to \infty$. When $\epsilon \to 0$, the problem reduces to the monodomain problem [8]. As shown by Roth [9], the main features of the solution can be understood in the limit $\epsilon \to 0$ by using perturbation theory, and at the zero order a dipolar contribution was found [10].

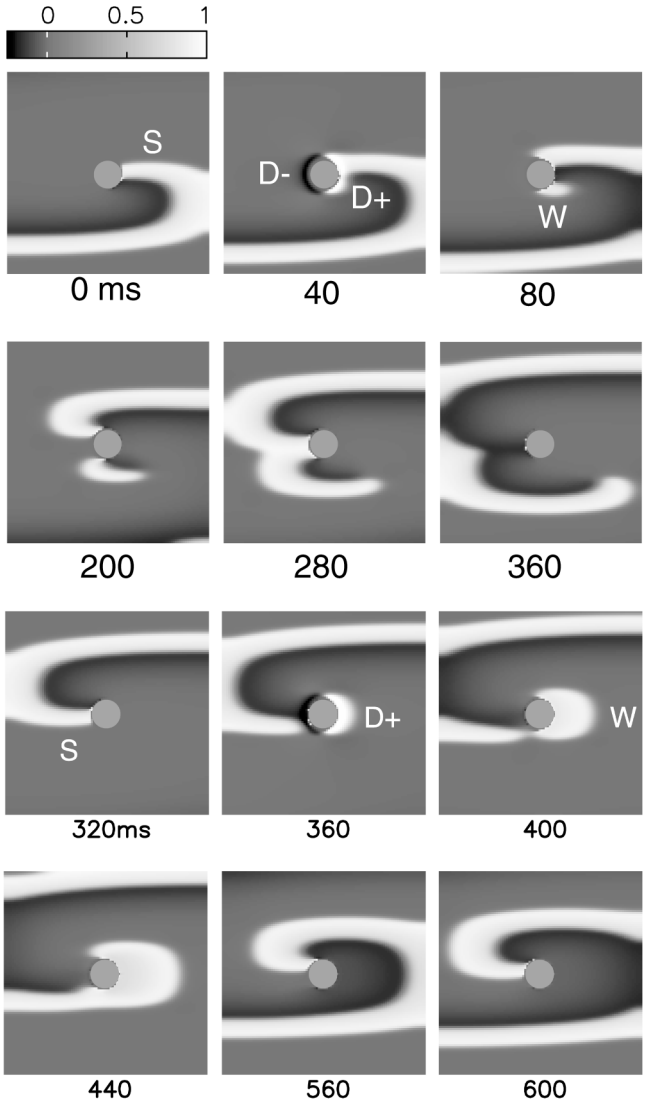

FIG. 2. Unpinning of a vortex: (a) unpinning. $t = 0$ ms, a pinned spiral rotating wave (S) . $t = 40$ ms, a dipole ($D-$, $D+$) is induced around the obstacle by an electric field (0.52 V/cm). $t = 80$ ms, a new wave W is created by $D+$. It propagates only clockwise (see $t = 200$ ms). $t = 280$ ms, collision of the wave W with the wave S. $t = 360$ ms, after annihilation of colliding parts, the rotating wave is unpinned. (b) No unpinning: $t = 320$ ms, a pinned wave (S). $t = 360$ ms, a dipole is induced. $t = 400$ ms, a new wave W is created by $D+$. It propagates in both directions. $t = 440$ ms, clockwise propagation merges it with S. The rotating wave is not unpinned ($t = 560$ ms, 600 ms). Parameters are the same as in [8], $dt = 0.2$ ms. FHN model, obstacle 12 mm diameter.

Expending the potentials in powers of ϵ, $\phi_e = \phi_e^0 + \epsilon\phi_e^1 + \ldots$, $V_m = V_m^0 + \epsilon V_m^1 + \ldots$, one can solve perturbatively Eqs. (3) and (4) at each order. At order zero, for $r \geq R$

$$\nabla^2 \phi_{e,\text{in}}^0 = 0; \qquad \nabla^2 V_m^0 - V_m^0/\lambda^2 = 0, \tag{5}$$

$$\nabla^2 \phi_{e,\text{out}}^0 = -V_m^0/\lambda'^2, \tag{6}$$

with $\lambda \equiv [(\Sigma_e + \Sigma_i)\beta G_m/(\Sigma_e\Sigma_i)]^{-1/2}$ and $\lambda' \equiv (\beta G_m/\Sigma_e)^{-1/2}$. The symmetry of the problem leads to a solution of the form $f(r) \times \cos(\theta - \theta_I)$, where θ_I is the angle between the fibers and the electric field. The membrane potential is expressed in terms of the modified Bessel function K_1: $V_m^0 = -\lambda E^0 K_1(r/\lambda)/K_1'(R/\lambda)$, whereas ϕ_e^0 behaves at large distances like $\phi_e^0 \sim (E_1 r + E_2/r)$. The constant $E^0 = I/(\Sigma_e + \Sigma_i) \times [1 - (1/2\lambda'^2) \int_R^\infty v_m^0(x)dx]$.

The first order correction satisfies

$$\nabla^2 V_m^1 - V_m^1/\lambda^2 + (\partial_x^2 - \partial_y^2)(\phi_e^0 + V_m^0) = 0, \quad (7)$$

$$\nabla^2 \phi_e^1 = -V_m^1/\lambda'^2. \quad (8)$$

The angular dependence of the forcing term in Eq. (7) implies that the solution has the following angular dependence: $f_1(r)\cos(\theta + \theta_I) + f_3(r)\cos(3\theta - \theta_I)$. The dominant contribution to the membrane potential at large distances can be readily obtained by noticing that the inhomogeneous term in Eq. (7) has a power law dependence, so $V_m^1(r, \theta) \sim \lambda^2/r^3 \times \cos(3\theta - \theta_I)$. This term decays algebraically, thus permitting the field to penetrate in the tissue at large distances [9,11].

The first order correction to the zero order, dipolar contribution, has a hexapolar structure [Fig. 1(c)]: its angular dependence has period $2\pi/3$. As it is the case for the "dog-bone" pattern, the $\epsilon \neq 0$ correction breaks the rotational symmetry of the problem, by bringing a quadrupolar contribution to the operator. Combining the dipolelike solution ($\cos\theta$) with the quadrupolar term ($\cos 2\theta$) in the operator leads to the appearance of $\cos 3\theta$ and $\cos\theta$ terms, i.e., a hexapolar structure. This is consistent with numerical results of [10].

We numerically simulated rotating waves in the full bidomain model Eqs. (2) and (3), with nonlinear ionic currents: the FitzHugh-Nagumo, and the Beeler-Reuter [12] model. The basic mechanism of unpinning can be understood from Fig. 2(a). We applied an electric field for 20 ms. Frame $t = 40$ ms shows the dipole ($D-$, $D+$) induced around the obstacle by the electric field. The hexapole components are not visible since the electric field is weak (0.52 V/cm) .

The positive part of the dipole $D+$ nucleates a new wave W ($t = 80$ ms). It propagates only clockwise. After colliding with the original rotating wave ($t = 280$ ms) and annihilation of colliding parts ($t = 320$–360 ms), the wave S is unpinned ($t = 360$ ms).

Note that symmetry breaking of the nucleated wave W (it propagates only clockwise) required proper timing of the electric pulse, just at the tail of wave S. With another timing, the nucleated wave W either propagates in both directions [Fig. 2(b)], or decays.

The correct interval of stimulation (called vulnerable window, VW) is determined by the condition that the image of the nucleated wave W in the phase space should contain the Maxwell point inside (see also [13]). A more evident interpretation is as follows: the nucleated wave W can propagate in only one direction if a part of its boundary has positive velocity (becoming a front of the wave) and another part has a negative velocity (becoming the tail of the wave). This condition sets both the time and the voltage limits of the unpinning window (see Fig. 4).

Other components of the hexapole pattern created by an electric field [Fig. 1(c)] can also induce unpinning. Naturally, they require larger electric field, since the hexapole components are smaller than the dipole components. The basic mechanism is the same: creation of a wave W colliding and annihilating with the pinned part of the rotating waves. An example is shown in Fig. 3.

Figure 4(a) summarizes the numerically observed unpinning mechanisms. The origin of the wave leading to unpinning (similar to W in Figs. 2 and 3,) is also indicated. Small electric fields $E > \sim 0.5$ V/cm unpin the vortex, in the time window $0 < t < 250$ ms; the wave interacting with the spiral originates from D_+. Outside this time window unpinning requires larger fields. For time $t < 0$ the wave W leading to unpinning originates from the hexapolar component H_2^+. For times $t > 250$ ms the waves originating from *several* components are involved, leading to a more intricate scenario (regions D–$H_2^+ D+$, D–$H_2^+ H_1^+$, D–$D+$). The main prediction of this work is the possibility to unpin with a low voltage; for the applications we have in mind, the branch $D+$ is the most relevant.

Unpinning was observed also in the ionic cardiac Beeler-Reuter (BR) model [12]. To optimize integration,

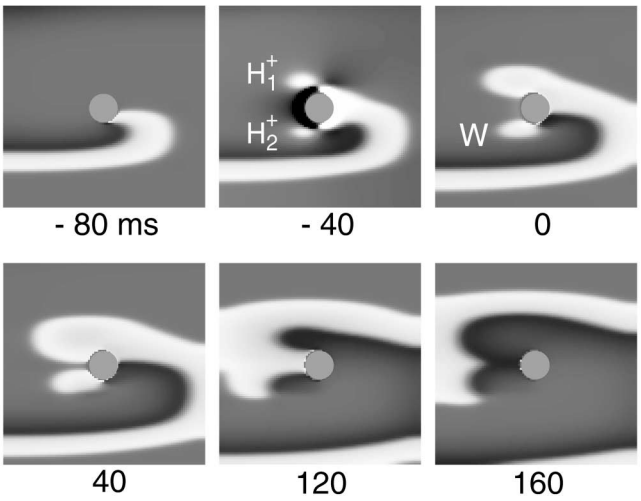

FIG. 3. A more complex scenario. $t = -80$ ms, a pinned wave S. $t = -40$ ms, both the dipole and hexapole components are seen, ($E = 4.5$ V/cm). $t = 0$ ms, a new wave W is created by the hexapole component H_2+; waves created by H_1+ and by $D+$ merge with S. Wave W propagates only clockwise ($t = 40$ ms). $t = 120$ ms, collision of waves W and S. $t = 160$ ms, the rotating wave is unpinned.

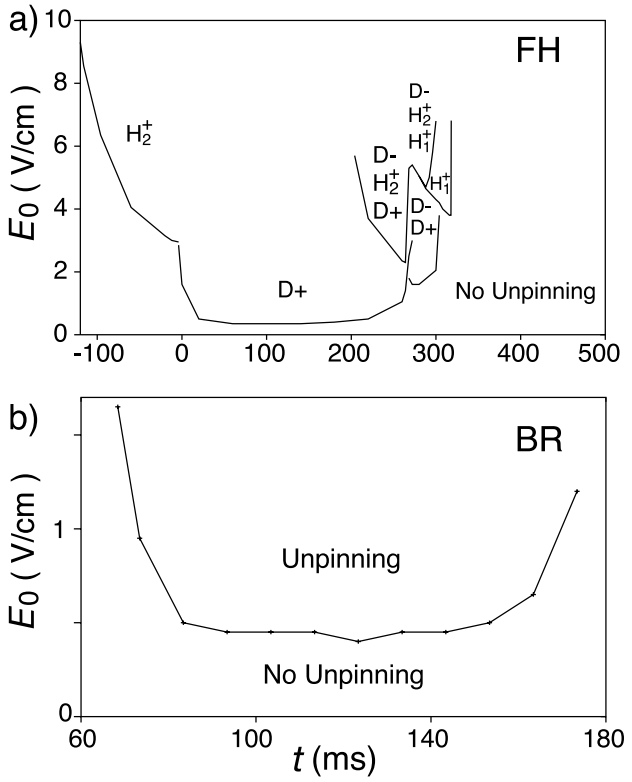

FIG. 4. The time window for unpinning. (a) FHN model. Components of the hexapole participating in unpinning are indicated near each branch. (b) cardiac BR model, low voltage part of the graph. Diameter of the obstacle 12 mm, period of rotation of the spiral wave $T = 222$ ms, duration of the electric shock 5 ms, anisotopy ratio $a = 4$, grid 200×200 elements.

the fast variable m, was treated adiabatically. This permitted us to use larger integration steps: $dt = 0.2$ ms, $dx = 0.15$ mm. The kinetics of activation of Ca current was increased 8 times to permit to work with small obstacles.

The low voltage part of the unpinning graph is presented in Fig. 4(b). It is seen that unpinning could be achieved with electric field <0.5 V/cm, or equivalently, with an energy $\sim$400 times less the defibrillation energy, and with a reasonably large time window, $\sim 1/2$ period of the rotating wave.

The optical mapping experiments on rabbit right ventricle confirmed main conclusions obtained here and will be published shortly in a cardiological journal.

In conclusion, we have found that an electric field creates a pattern of membrane polarization localized around an obstacle in cardiac tissue. Thus, unpinning or removal of rotating waves can be achieved. The energy needed is 2 orders of magnitude less than defibrillation energy. Importantly, the knowledge of the position of the pinned vortex is not needed. This opens a way to new manipulations with pinned vortices both in experiments and in cardiac clinics.

The work was supported by INRIA (France), by European Contract No. HPRN-CT-2002-00312, and by the American Heart Association. It is a pleasure to acknowledge discussions with N. Otani and S. Kanani.

*Electronic address: alain.pumir@inln.cnrs.fr
†Electronic addresse: ire@cwru.edu

[1] U. Frisch, *Turbulence* (Cambridge University Press, Cambridge, 1995).
[2] P. G. de Gennes, *Superconductivity of Metals and Alloys* (Addison-Wesley, Reading, MA, 1966).
[3] F. Dalfovo *et al.*, Phys. Rev. Lett. **85**, 1028 (2000).
[4] R. Blaauwgeers *et al.*, Nature (London) **404**, 471 (2000).
[5] D. A. Butts and D. S. Rokhsar, Nature (London) **397**, 327 (1999).
[6] D. Hayes, M. Lloyd, and P. Friedman, *Cardiac Pacing and Defibrillation: A Clinical Approach* (Futura, Armonk, NY, 2001), p. 318
[7] B. J. Roth and J. P. Wikswo, Jr., IEEE Trans. Biomed. Eng. **33**, 467 (1986).
[8] A. Pumir and V. I. Krinsky, J. Theor. Biol. **199**, 311 (1999).
[9] B. J. Roth, Phys. Rev. E **55**, 1819 (1997).
[10] D. Langrill and B. J. Roth, IEEE Trans. Biomed. Eng. **48**, 1207 (2001).
[11] N. F. Otani, IEEE Trans. Biomed. Eng. (to be published).
[12] G.W. Beeler and H. Reuter, J. Physiol. **268**, 177 (1977).
[13] F. Starmer *et al.*, Biophys. J. **65**, 1775 (1993).